Summertime Rainfall Events in Eastern Washington and Oregon

ANDREW M. CHIODI AND NICHOLAS A. BOND

Joint Institute for the Study of the Atmosphere and Ocean, University of Washington, and NOAA/Pacific Marine Environmental Laboratory, Seattle, Washington

NARASIMHAN K. LARKIN AND R. JAMES BARBOUR

Pacific Northwest Research Station, U.S. Forest Service, Portland, Oregon

(Manuscript received 10 February 2016, in final form 6 July 2016)

ABSTRACT

The temporal and spatial characteristics of summertime rainfall events in the Pacific Northwest are examined in relation to the prevailing regional 500-hPa geopotential height conditions, with focus on the forested slopes of eastern Washington and northeastern Oregon, where the absence/occurrence of events largely determines the start and end of the wildland fire season. The Daily U.S. Unified Precipitation dataset is used for specifying rainfall events (period 1949–2008). Events are defined as one or more consecutive days of rainfall exceeding 0.25 in. (0.65 mm), and occur on average two to three times per summer (July–September) in the focus region, east of the Cascade Mountain crest, with a minimum in frequency in late July. A relatively high percentage of the events in the northern portion of the domain of interest, and over the higher terrain, is associated with anomalous midtropospheric southwesterly flow; a high percentage of the events in the southern and lower elevation portions of the domain is associated with southeasterly flow anomalies. Southeasterly flow events are much more likely to be accompanied by lightning and a more localized rainfall distribution than southwesterly events. Southwesterly events mainly account for the late-July frequency minimum and produce more widespread/heavier precipitation on average. The forests of eastern Washington and Oregon receive a mix of southeasterly and southwesterly events. Results suggest that identifying flow types by (skillful) extended-range 500-hPa forecasts may provide a useful basis for predicting the associated aspects of the rainfall event distribution.

1. Introduction

Summertime rains that occur in the Pacific Northwest, east of the Cascade Mountain crest, provide a useful boost to soil moisture for agriculture in eastern Oregon and Washington and important increases in streamflow once snowmelt runoff is depleted. Variations in summertime precipitation amounts, and especially their contribution to the curing of live, and drying of dead fuels (Abatzoglou and Kolden 2013), have been linked to interannual changes in the forested area burned by wildfire over this region (Littell et al. 2009). Summertime rains also play a critical role in determining the timing of the region's wildland fire season; rain events that occur in the early summer often serve to postpone the start of the fire season, whereas a rain event in late summer/early fall can effectively end that threat. Despite their substantial importance to the region's ecology, however, relatively little effort has been directed toward diagnosing summertime precipitation in the Pacific Northwest east of the Cascade Mountains. The authors are not aware of another study that examines summertime precipitation events over this region the way this one does.

The storms that occur regularly on the west side of the Cascades during the cool season are often associated with damaging floods, and have been better studied than the summertime events we examine here. Previous examinations of the region's cool-season precipitation events

Denotes Open Access content.

Supplemental information related to this paper is available at the Journals Online website: http://dx.doi.org/10.1175/WAF-D-16-0024.s1.

Joint Institute for the Study of the Atmosphere and Ocean Contribution Number 1888 and Pacific Marine Environmental Laboratory Contribution Number 3755.

Corresponding author address: Andrew M. Chiodi, JISAO/University of Washington, Box 354925, Seattle, WA 98195-4925.
E-mail: andy.chiodi@noaa.gov

DOI: 10.1175/WAF-D-16-0024.1

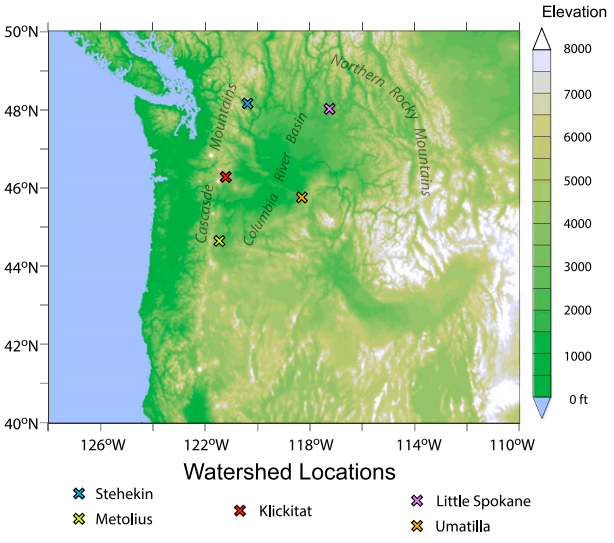

FIG. 1. Study region topography showing watershed site locations.

have identified the poleward transport of subtropical moisture (Lackmann and Gyakum 1999) and associated high levels of vertically integrated water vapor (e.g., Neiman et al. 2008, 2011; Rutz et al. 2014, Warner et al. 2012) as important precursors to heavy cool-season rains. Such conditions are characteristic of the atmospheric river events studied by Parker and Abatzoglou (2016), which were found to be a prominent source of cool-season precipitation, especially over the western slopes of the Cascade Mountains. The statistical connection between high precipitable water amounts and rain events, however, has been found to be much weaker in summer than winter, with precipitable water amounts being frequently high in summer, even in times with no appreciable rain (Warner et al. 2012). Abatzoglou et al. (2016) found that about a third of the region's total summertime rainfall is linked to nearby cutoff lows in the prevailing upper-tropospheric circulation. Nevertheless, a more complete understanding of the range of conditions that are conducive to summertime rainfall events is needed.

The regional geography is characterized by the largely north–south-running coastal Cascade Mountain range, east of which lie the lower elevations of eastern Oregon and Washington's Columbia River basin. Moving farther east, these lower elevations rise to meet the foothills of the greater Rocky Mountains (Fig. 1). The climatological summertime-average midtropospheric (500 hPa) circulation is westerly with a magnitude of about $10\,m\,s^{-1}$ over this region (which is less than the wintertime mean by about 50%). Regional flow anomalies in the zonal direction translate directly into broad-scale modulation of upslope flow (orographic lift) across the western faces of the Cascade Mountains, and precipitable water amounts are generally much higher over the adjacent North Pacific Ocean than land. The circulation aloft has traditionally been used to characterize regional flow patterns, and is known to regional forecasters and meteorologists to have a usefully strong connection to local weather conditions (e.g., Lackmann and Gyakum 1999). Rorig and Ferguson (1999) found 500-hPa flow useful for discriminating between wet versus dry thunderstorm days in the Pacific Northwest.

Here, we examine the distribution of summertime rain events and their relationship to the regional atmospheric circulation in terms of 500-hPa geopotential height anomaly patterns. Our main focus is on the forests of the interior Pacific Northwest that surround the Columbia River basin. Since the existing precipitation frequency atlases (e.g., Bonnin et al. 2011) are not stratified by season, we first revisit the frequency distribution of summertime rainfall events, then systematically examine its relationship to regional flow conditions, focusing first on the regional flow anomaly direction, and then also considering the effects of flow strength. We define rainfall events as a day, or consecutive days, with >0.25-in. (0.65 mm) daily average precipitation. The 0.25-in. threshold is one associated with the current practical definitions for rainfall events sufficient to curtail the threat of wildland fire in the focus region.

Using the direction of the anomalous (500-hPa geostrophic) flow over the Columbia basin to characterize the regional atmospheric circulation, we examine the associated rainfall event characteristics for aspects (e.g., differences in spatial distribution patterns, seasonality, likelihood of lightning co-occurrence) favored by different flow anomaly regimes. The regional circulation associated with particular types of weather events is often evaluated by compositing circulation at the times of the events. The approach taken here can be thought of as a complementary one to the traditional event-compositing method, in that, here we identify periods of interest based on the regional flow characteristics and then examine the characteristics of the precipitation during events occurring in the different flow regimes. One motivation for choosing this approach is that we are interested in learning more about the extent to which ongoing efforts to provide skillful regional flow forecasts (e.g., the 6–10- and 8–14-day 500-hPa geopotential height "outlooks" available from the NOAA/CPC) might provide complementary information for the direct precipitation forecasts.

We also consider a complementary set of results based on day-to-day increases in the streamflow of five unregulated rivers located in the region of interest (forested slopes east of the crest of the Cascade Mountains) with watershed drainage areas about the size of the

0.25° latitude × 0.25° longitude precipitation grid boxes. Day-to-day rises in streamflow that occur during the summer, after the previous winter's snow has melted, offer an independent indication of rainfall in these watersheds, and provide an opportunity to compare the atmospheric circulation patterns keyed on precipitation events with those keyed independently on streamflow increases. We also examine the effects that the identified precipitation events have on day-to-day changes in streamflow.

2. Data and methods

The Daily U.S. Unified Precipitation dataset from the NOAA/CPC (NOAA 2008; Higgins et al. 2000) is used to identify and characterize precipitation events. The dataset was obtained from the NOAA/OAR/Earth System Research Laboratory(ESRL)/Physical Sciences Division (PSD), Boulder, Colorado (available at http://www.esrl.noaa.gov/psd) and employs a Cressman-type objective analysis to provide daily values of precipitation based on station data on a grid with a spacing of 0.25° latitude/longitude. The recent development of gridded precipitation datasets on daily time scales makes our analysis feasible, since direct station observations are sparse in the region of interest (Guirguis and Avissar 2008). Rainfall events are primarily defined herein based on the days in July, August, or September with daily average rainfall above 0.25 in. Consecutive days that meet these criteria are counted as a single event that lasts until the daily average rainfall dips below 0.25 in., but most events last a single day. We consider the 60-yr period from 1949 through 2008 and have estimated the expected 20-yr maximum daily average summertime event rainfall directly from the 60-yr record (i.e., third largest summertime event at each location).

The atmospheric circulation anomaly patterns associated with the precipitation events are specified in terms of maps of 500-hPa geopotential height anomalies. Lower (higher) than normal heights in the Northern Hemisphere imply counterclockwise (clockwise) geostrophic circulation along the negative (positive) geopotential height anomaly contours. Geopotential height information was obtained from the National Centers for Environmental Prediction–National Center for Atmospheric Research (NCEP/NCAR 1996) reanalysis dataset (Kalnay et al. 1996) wherein such data are provided on a 2.5° latitude × 2.5° longitude grid and available at a four-times-daily resolution. Based on the four-times-daily data, we consider averages over the 24-h periods during which the rainfall accumulations are reported in the precipitation dataset (1200–1200 UTC). Anomalies are determined based on linear interpolation of the monthly averaged climatology, using the full study period (1949–2008) as the baseline.

Daily streamflow data are acquired from the U.S. Geological Service (USGS 2009) for five rivers across the study area: the Stehekin, Klickitat, Metolius, Little Spokane, and Umatilla Rivers (Fig. 1). Each watershed is located east of the Cascade Mountain crest and features the forest habitat for which information on summer rainfall is of particular interest. The streamflow records from three of these five rivers span the entire period considered. There are gaps amounting to 20% and 50% of the 1949–2008 record length in the Klickitat and Little Spokane streamflow records, respectively. Each of these rivers is unregulated and fed by a drainage area comparable in size to the 0.25° latitude × 0.25° longitude precipitation grid boxes. In the streamflow case, events are identified based on day-to-day increases in streamflow, with thresholds chosen to yield a similar number of events per year as rainfall. Days immediately following large/abrupt increases in temperature (>5°C) are neglected to avoid the influence of possible glacier melt.

We also examine information on lightning strikes contained in the U.S. National Lightning Detection Database (NLDN 2002) for the likelihood of their co-occurrence with the different flow/rainfall event types. To do this, we aggregated the available list of lightning strikes onto the 0.25° latitude/longitude grid of the precipitation data. Although a single lightning strike is by no means a sufficient condition for a fire start in this region, lightning has nonetheless been found to be a dominant source of fire ignition over the mountainous Pacific Northwest (Abatzoglou et al. 2016). Because the lightning data available to us cover only a small portion (2002–07) of the 60-yr rainfall study period, we identify precipitation events using a lower rain event threshold (0.1 in. day^{-1}) in this case.

To examine the effects that midtropospheric flow anomalies have on the distribution and likelihood of rainfall, we begin by grouping the possible flow anomaly directions into eight prescribed sectors, based on the direction of the anomalous daily 500-hPa geostrophic flow averaged over the box extending from 44° to 49°N and 122° to 117°W; this box roughly comprises the greater Columbia River basin and its forested flanks of interest. Preliminary investigation at the five selected watershed sites revealed that using the flow directions taken from the grid boxes containing the specific watershed locations (rather than using the Columbia basin box average) produces very similar results, so we only discuss the box-averaged results herein. The results remain qualitatively unchanged when using boxes that are shifted south by 1°–2° latitude. Although our core results remain the same regardless of whether flow direction is based on the box-average or individual site location, the

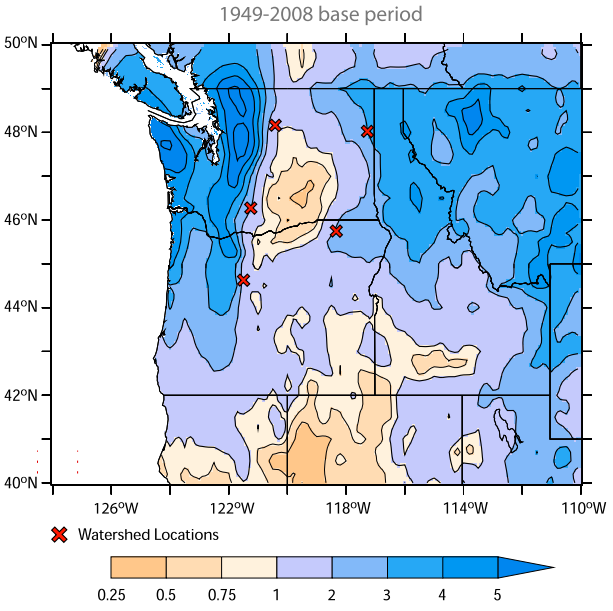

FIG. 2. Climatological average number of rainfall events per summer (July–September).

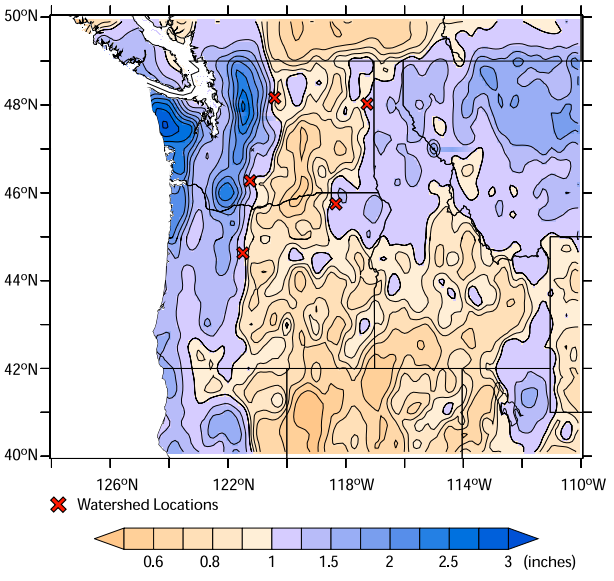

FIG. 3. Estimated maximum daily average event precipitation during summer over a 20-yr return period.

use of daily averages means this method is suited for understanding the effects of the regional atmospheric circulation on larger scales (roughly >500 km). The eight flow direction sectors are prescribed such that a line running north–south constitutes one dividing line (to mirror the basically north–south orientation of the Cascade Mountain crest) and each sector subtends an angle of 45° (as represented in the subset icons in Fig. 4). Events are thereby categorized by their anomalous flow direction in a manner that can be automated/replicated. We use eight sectors initially to compare the associated rainfall distributions at a granularity fine enough to detect at least broad-scale changes in the rainfall distribution characteristics, while still having enough events in each sector to yield useful levels of statistical reliability. Commonalities between subsets of the eight-sector results (as discussed below) lead us to present results based mainly on three separate anomalous flow-direction categories. In this case, the two most northerly sectors are joined to form one group (''northerly''). The remaining three sectors with a westerly flow anomaly component form another group (''southwesterly'') and the remaining three sectors with an easterly component form the third category (''southeasterly'').

In subsequent analyses, we also consider the effects of flow anomaly strength on the rainfall distribution. For our purposes, flow strength is determined relative to the average geostrophic (500 hPa) wind speed anomaly seen for all days in which the flow is in the given direction category. For example, a daily averaged northerly flow anomaly is considered weaker than average when its magnitude is less than the average magnitude computed over all days with northerly flow (i.e., flow from 315° to 45° nautical, including due north at 0°/360°).

3. Summertime average rainfall

We begin with a regional map of the average number of rainfall events (day, or consecutive days, with >0.25-in. accumulation) per summer (July–September; Fig. 2). This distribution is very closely related to that of the terrain. Rainfall events are most frequent just to the west of the crest of the Cascade Mountains (along ~122°W) from central Washington into southern British Columbia, where fewer than five such events occur each summer, on average. Event frequency is also enhanced (e.g., usually three or more events per summer) along the higher east-facing slopes of the Cascades, and other mountainous regions of the interior Pacific Northwest. The five selected watersheds experience from slightly fewer than two [Stehekin and Metolius; streamflow gauge elevations ~335 m (1100 ft) and 600 m (1975 ft), respectively] to about three [Little Spokane; elevation 560 m (1840 ft)] rainfall events per summer, on average. The fewest numbers of rainfall events tend to occur each summer in the lower elevations of the Columbia River basin in eastern Washington and Oregon. Rain events are more likely at higher than lower elevations in this region.

A similar (but certainly not identical) pattern is found for the expected 24-h maximum rainfall event over 20 summers (Fig. 3; cf. Miller et al. 1973). In particular, the

estimated magnitude for this parameter is approximately 1 in. for all five watersheds, with less of a propensity for wetter conditions in the north, as compared with the previous distribution with respect to frequency. In this case, the western slopes of the Cascade Mountains in Washington (along with the western slopes of the Olympic Mountains on Washington's Olympic Peninsula) stand out as the locations within this region with the most intense summertime rains.

4. Distribution by flow direction

Next, we consider how the rainfall event days are distributed with respect to the regional midtropospheric (500-hPa geostrophic) flow direction. Systematic examination of eight flow sectors reveals that the rainfall frequency distribution clearly changes with flow direction over this region (Fig. 4; the pie charts in each panel show the source direction of the anomalous flow). Although northerly and southerly flow direction anomalies are almost equally probable in this region (Fig. 4; percentages next to pie charts), the more southerly flow directions account for a much greater share of the rainy days over the vast majority of the locations considered, whereas heavy rains are rare in this region when the anomalous flow is from the north. There are also notable differences in the character of the distributions, depending on whether there is an easterly or westerly component in the anomalous flow. The westerly cases account for most of the rainfall event days in the Cascade Mountain range (including eastern slopes), along with nearly half of the rainy days in the higher elevations of eastern Washington and northeastern Oregon/Idaho. Easterly flow anomalies, and especially flows out of the south-southeast to east-southeast directions, are especially conducive to rain events in the lower elevations of the Columbia basin, as well as the high plateaus of eastern Oregon and the more southern portions of the study domain.

The relative scarcity of rainy days in northerly flow anomaly conditions, along with the near-mirror-image relationship between the easterly and westerly cases, suggests a three event-type grouping, which we (mainly) adopt to summarize our results hereafter. The three aforementioned flow categories in this case are: 1) northerly, composed of the two sectors with anomalous flow coming from nearly due north, during which rainfall events are rare; 2) southwesterly, composed of the westerly to south-southwesterly sectors, which largely dominates the event distributions at higher elevations; and 3) southeasterly, which accounts for most of the regions' lower-elevation rainfall flow conditions. Mapping the distribution of the rainfall event frequency based on these three flow categories (Fig. 5) summarizes how the rainfall distribution character changes with flow direction, and illustrates the distinction between the rainfall distribution patterns associated with southwesterly and southeasterly type events.

5. Chances of rain based on flow direction and strength

Here, we examine the basic effects of the regional flow anomaly direction and strength on the distribution of rainy days. In this case, flow strength is determined relative to all summer days with flow in the given direction category (as described in section 2). When the flow anomaly strength is weaker than average and either northerly or southeasterly in origin, rainy days are infrequent (less than 5% chance per day) everywhere in Washington and Oregon (Fig. 6, top panels; northerly case not shown for brevity). In weak southwesterly flow, chances remain less than 5% everywhere except in the Cascade Mountains and coastal mountains (mainly in Washington), where up to 15% of the weak southwesterly flow days receive >0.25 in. of precipitation at the highest elevations. To provide context for precipitation changes by flow direction and strength, we normalize the observed chance of precipitation during weak flow days by the overall chance of summertime precipitation (irrespective of flow direction). Results show that weak flow anomalies in each direction are associated with normal (e.g., southwesterly case over the Cascade Mountains) to less than normal (especially in the northerly case) chances of rain over this region (Fig. 6, bottom panels).

When flow anomalies are stronger than average (Fig. 7, top panels), enhancements occur in the higher elevations during strong southwesterly flow, with about a third of such days having >0.25 in. of rain along the crest of the Cascade Mountains in northern Washington. Strong southwesterly flow is also associated with more modest enhancements along the Cascade crest, as well as the Rocky Mountains of Idaho and Montana. Normalizing by the overall chance of seeing rain (Fig. 7, middle panels) in this case reveals that strong northerly flow makes rainy days even more rare than usual (factor of 4, or more, over much of the focus region; not shown for brevity), whereas strong flow from the southwest (southeast) mainly favors rainfall over the higher (lower) elevations of the Columbia River basin, with chances of seeing a rainy day in this flow condition two to three times greater than average. We also examined this aspect of the rainfall distribution based on the initial eight flow sectors and find particularly sharp enhancements/reductions (up to a factor of 7) for the cases with flow from the directions just south of east and west (Fig. 7, bottom panels).

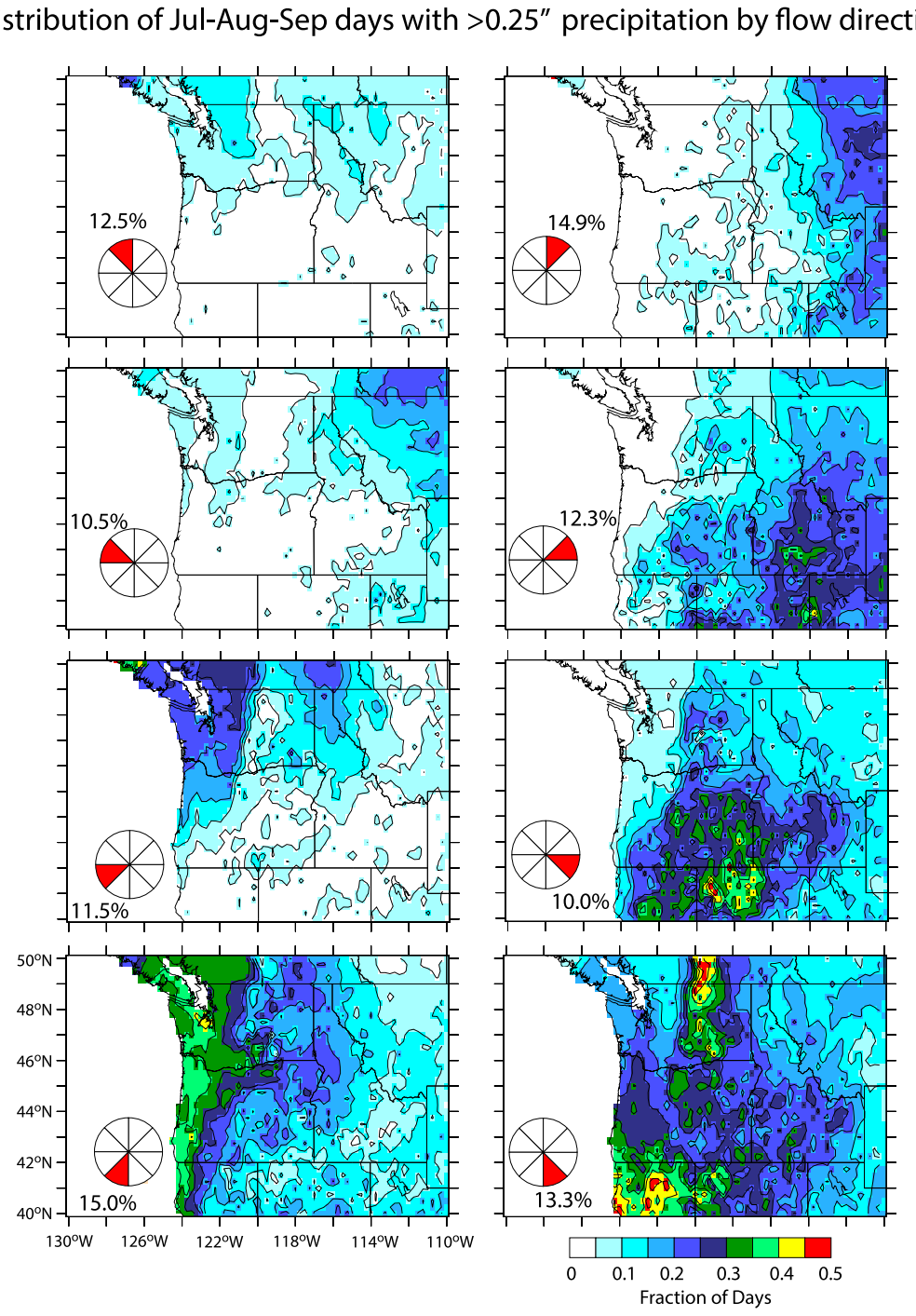

FIG. 4. Distribution of summertime "rainy days" (daily rainfall > 0.25 in.) by regionally averaged 500-hPa flow direction. The flow-averaging region in this case is 43°–48°N, 122°–117°W. Base period is 1949–2008.

6. Precipitation event seasonality

The seasonal cycle during rainfall events, coded with respect to circulation type, is plotted for the five watersheds in Fig. 8. Events are relatively rare in late July at all six locations. The three western locations (Stehekin, Klickitat, and Metolius) tend to experience more wet days in early fall (mid-September–early October) than in late spring (June); the two eastern locations (Little Spokane and, to a lesser extent, Umatilla) have wet days

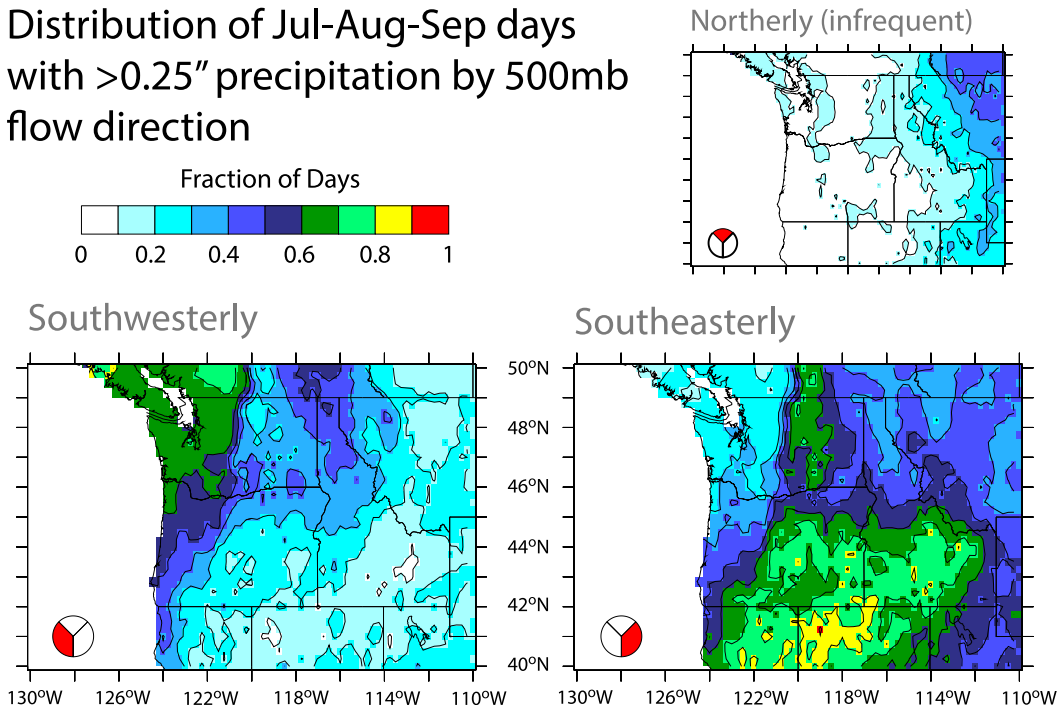

FIG. 5. As in Fig. 4, but for three flow-direction categories.

more frequently in late spring than in early fall. In general, the seasonality is relatively pronounced with respect to the southwesterly events, and is manifested to a lesser extent with respect to southeasterly events. Thus, it is mainly the cessation of southwesterly events in late July, perhaps associated with the seasonality of the general circulation and the storm track reaching its northernmost and weakest point, which accounts for the minimum in total rainfall events seen at this time of year.

7. Lightning associations

The distribution of lightning accompanying the rainfall events is strongly dependent on circulation type. As mentioned in section 2, this portion of the analysis is limited to observations for the period of 2002–07 and the precipitation event threshold in this case was reduced (to 0.1 in.) so that more than just two or three events, on average, per summer are identified in the focus region. The composite lightning distributions for the rainfall event days in this case are shown in Fig. 9 (top panels; northerly case not shown for brevity). Very few lightning strikes occurred in the western portions of Washington and Oregon in all three flow categories. Lightning was much more prevalent, and occurred with greater strike density (i.e., strikes per grid cell per day) during southeasterly circulation events. These southeasterly case enhancements are apparent over the Cascade Mountains but are especially strong to their east in the region of the lower terrain of the Columbia basin. A complete analysis of the cause(s) for the more frequent lightning during the southeasterly events is beyond the scope of the present paper. Our results are consistent with those of van Wagtendonk and Cayan (2008), who found that easterly wind anomalies at 700 hPa corresponded with a greater frequency of summertime lightning in California.

It bears emphasizing that, whereas the southeasterly events feature relatively more lightning, the southwesterly circulation types generally include greater rainfall amounts, especially over the higher terrain. We further examined the distribution of days in which lightning strikes occurred but little to no rainfall (<0.1 in.) was seen. Such, dry-lightning conditions were much more frequent during the southeasterly events (Fig. 9, bottom panels) than the southwesterly or northerly events. These results are consistent with the findings of Rorig and Ferguson (1999) regarding conditions favoring "dry" versus "wet" lightning in the interior Pacific Northwest. Moreover, since it is the southeasterly events that are the dominant cases in midsummer when fuels are typically near their driest conditions, this type of flow event is more conducive to the natural ignition of wildfires than are the other circulation types.

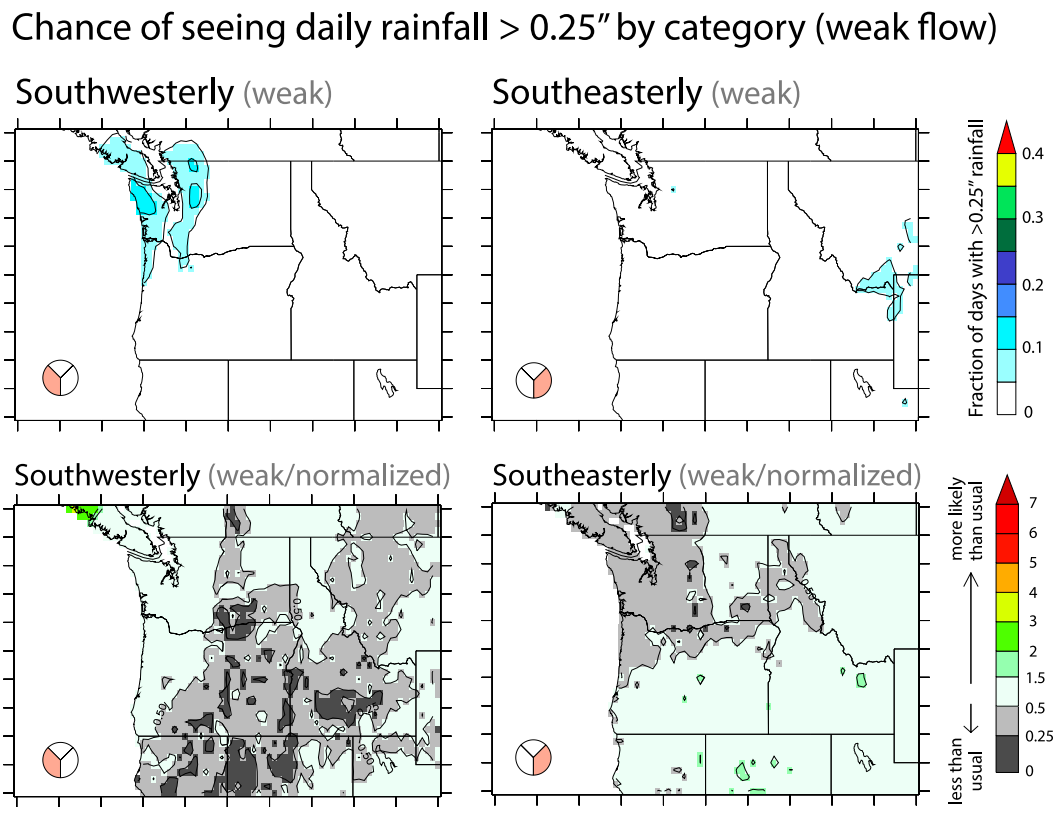

FIG. 6. Rainfall (>0.25 in.) likelihood by flow category. (top) The ratio n/t, where n is the number of (July–September) days in a given flow category with daily average rainfall > 0.25 in., and t is the total number of days in that category. Only weak flow conditions (for their respective categories; see text) are considered in this case. (bottom) The same ratio as in the respective top panel, but normalized by the overall ratio N/T, where N is the total number of days at a grid point with rainfall > 0.25 in. (irrespective of flow direction) and T is the total number of days (July–September) considered.

8. Basic circulation patterns

a. Keyed on precipitation

The 500-hPa geopotential height anomaly patterns for the precipitation events at the selected river sites are described here, based on the three flow regimes identified in section 4. To allow an independent look at the regional flow patterns associated with large summertime streamflow increases, we computed maps based on river and rainfall events for each of the five river sites (using the precipitation grid box closest to the site since the drainage area is comparable in size), but include figures only for the Klickitat site here, since their counterparts for the four other sites, at least in the case of the more frequent southwesterly and southeasterly events, are virtually identical.

The composite circulation patterns, based on rainfall events at the Klickitat River site, are shown in the top panels in Fig. 10. The southwesterly circulation pattern has a negative anomaly center (dashed contours) near 51°N, 133°W and a region of positive anomalies (solid contours) stretching from the date line to the West Coast, south of 45°N. In the southwesterly case, broad portions (~10° × 10°) of these two anomaly patterns are statistically significant at the 95% confidence level (based on a two-tailed Student's t test) and robust, in the sense that a large fraction of the individual days considered in the composite (>80%) have an anomaly of the same sign as the one seen in the composite average (shown by shading in Fig. 10). The 500-hPa heights are lower than normal in these situations over the particular site being keyed upon.

The southeasterly circulation pattern exhibits a statistically significant and robust mean 500-hPa height anomaly distribution with a negative center of about 100-m magnitude on or just west of the Oregon coast at 42°–45°N, and positive anomalies to the northeast over Alberta, Canada (Fig. 10). It deserves mention here that the southeasterly flow anomaly in this case, in combination with the climatological mean (westerly) flow, yields an average resultant flow during these events from the south-southwest. We performed a review of backward

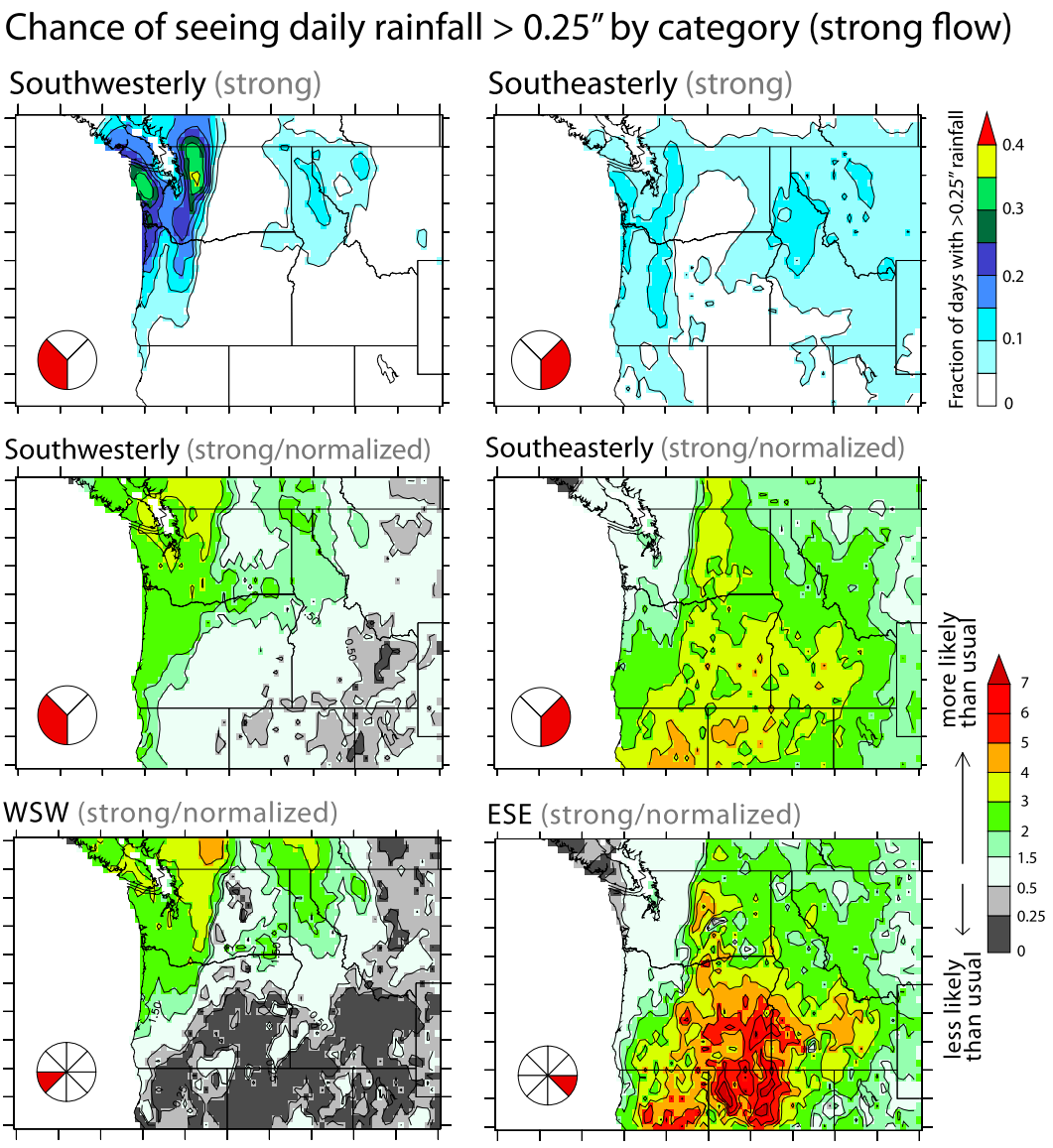

FIG. 7. (top),(middle) As in Fig. 6, but for strong flow conditions. (bottom) As in the middle row, but based on the two of eight sectors just south of due east and due west, i.e., west-southwesterly (WSW) and east-southeasterly (ESE).

trajectories over 48-h periods for a variety of individual events using the HYSPLIT application provided by NOAA's Air Resources Laboratory (http://www.arl.noaa.gov/HYSPLIT_info.php). We focused on southeasterly events and found that the lower- to middle-tropospheric air at the site being keyed upon often originated from northern California (not shown for brevity).

The northerly events are different from the other two categories in that they are associated with a negative 500-hPa height anomaly center located inland, near 45°N, 110°W (not shown for brevity). One might suppose that these types of events frequently follow southeasterly events as a result of the eastward propagation of a 500-hPa low across the Pacific Northwest, but inspection of the time-lagged composites over several days suggests that this is not generally the case. Instead, it appears that each type of event is much more likely to be associated with essentially in situ development.

b. *Keyed on streamflow*

The set of maps keyed on river increases is very similar to those that keyed on rain events, especially for the southeasterly and southwesterly cases (Fig. 10, bottom panels), confirming that the circulation patterns associated with heavy summertime rains in these cases are also

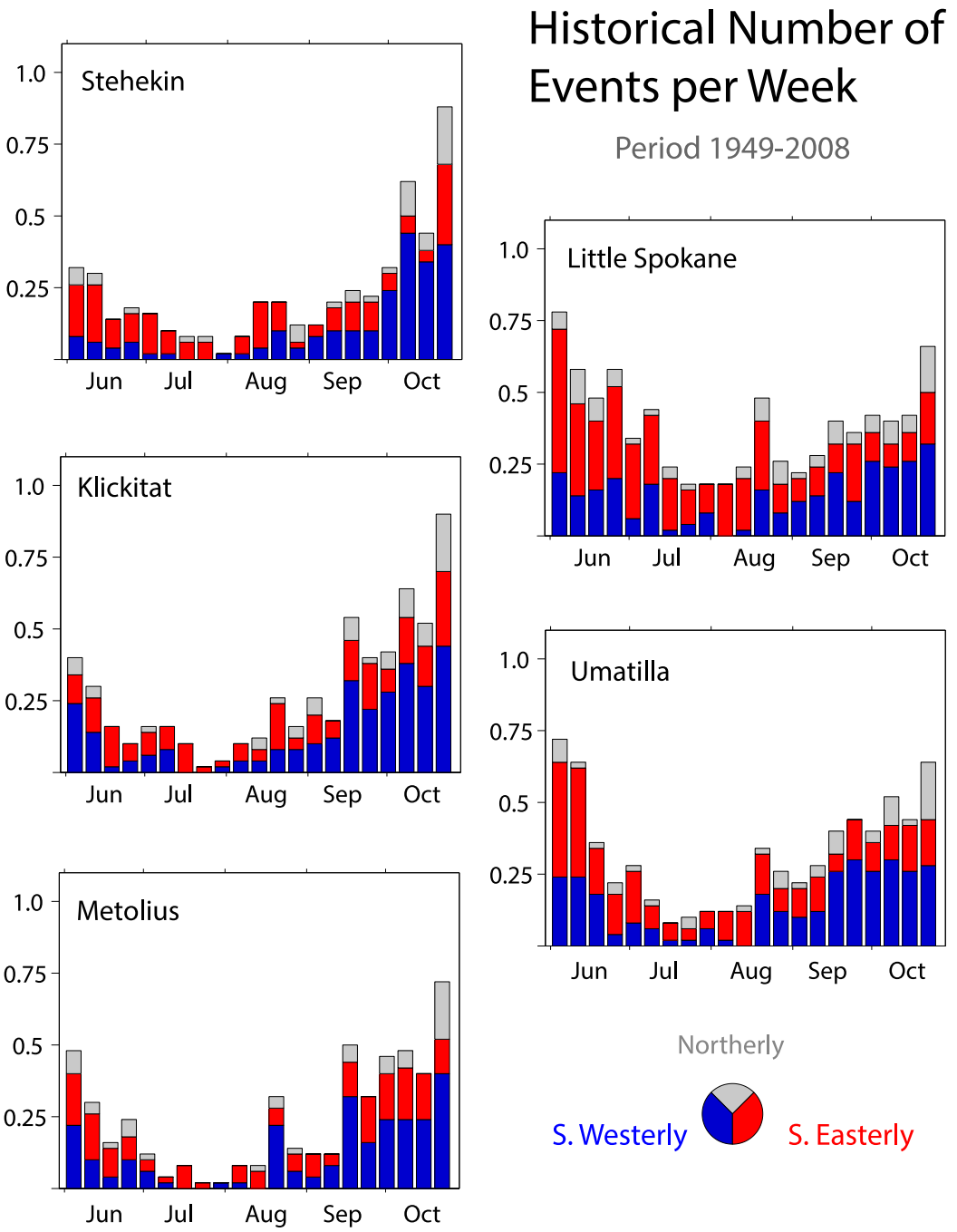

FIG. 8. Climatological number of >0.25-in. rainfall events by week and flow-direction category. Note that seasonal changes in the numbers of southwesterly events mainly determine the shape of the total seasonal cycle.

associated with day-to-day increases in streamflow in the region of interest. In the Klickitat case, river events are identified based on a day-to-day streamflow-increase threshold that yields a comparable number of events as in the precipitation event case. This threshold is 15 cubic feet per second (cfs) per day, in this case, which is roughly the 97th percentile value. The overall summertime-averaged day-to-day change is $-3.5\,\text{cfs}\,\text{day}^{-1}$ at this site, and the mean summertime streamflow is 174 cfs.

In the Klickitat case, 57% of the precipitation events identified over the watershed location are accompanied by day-to-day streamflow increases of >1 standard deviation (~13 cfs). For the Little Spokane, this percentage rises to 74%. The average day-to-day

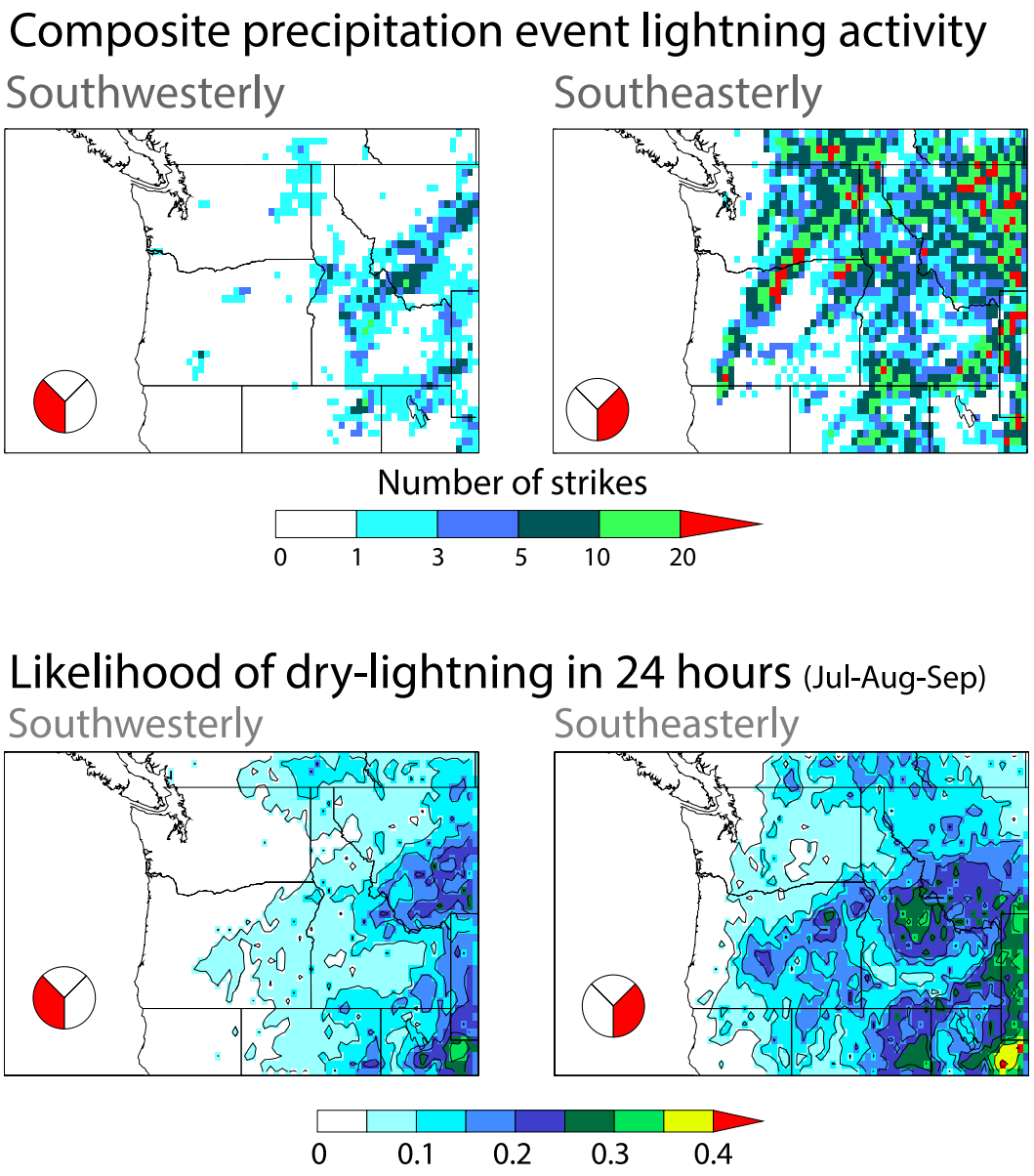

FIG. 9. (top) Composite average number of lightning strikes during (left) southwesterly and (right) southeasterly type precipitation event days, based on events occurring at any of the five selected watershed sites. (bottom) Likelihood of lightning accompanying days with daily rainfall < 0.1 in. Shown is the ratio nd/nt, where nd is the number of dry days, by flow category, at a given grid point with at least one lightning strike, and nt is the total number of days in that flow category.

change in streamflow associated with precipitation events at the Klickitat site was $+23\,\text{cfs}\,\text{day}^{-1}$, which is statistically significant at the 99% confidence level. Peak increases reached up to $100\,\text{cfs}\,\text{day}^{-1}$, or about half of the mean summertime flow (174 cfs). Although they scale with the respective mean streamflow (ranging from a summertime mean of 46 cfs in the Little Spokane River case, to ~1600 cfs in the Stehekin River case), the average daily streamflow changes associated with the identified precipitation events are statistically significant (at 99%) and positive, for each of the five selected watersheds.

9. Composite event precipitation patterns

The mean distribution of daily average rainfall associated with precipitation events is illustrated here, based on events during the southwesterly and southeasterly atmospheric circulation regimes (we omit the rare northerly case) at the Klickitat and Little Spokane

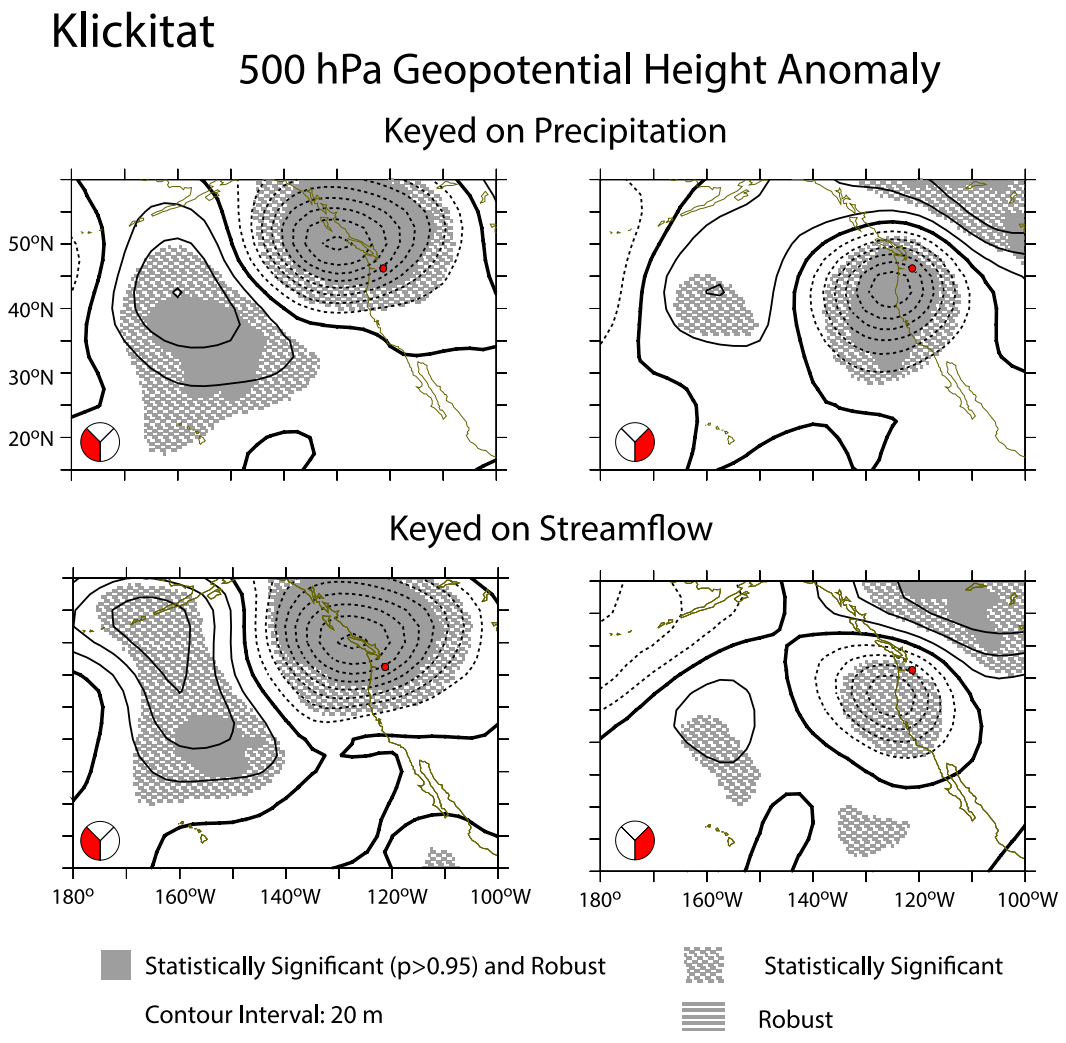

FIG. 10. (top) The 500-hPa geopotential height anomalies (m; negative values shown with a dashed line) associated with the three regional circulation categories (see text for definitions) keying on rainfall events (daily totals > 0.25 in.) in the Klickitat River watershed. The sectors for the anomalous 500-hPa flow associated with each category are indicated by pie charts in the lower-left corner of each panel. Anomalies are shaded where statistically significant (based on a two-tailed Student's *t* test) and "robust," meaning in this case that at least 80% of the composited events have anomalies of the same sign. The composites shown are based on 74, 44, and 9 events for the southwesterly, southeasterly, and northerly (not shown) types, respectively. (bottom) As in the top panels, but keyed on streamflow events (daily increase > 1.2 normalized standard deviations) on the Klickitat River, and based on 57, 37, and 9 July–September events for type southwesterly, southeasterly, and northerly (not shown) atmospheric circulation patterns, respectively.

watershed sites. The sets of maps for the other three locations are quite similar, respectively (e.g., Stehekin and Metolius resemble Klickitat; Umatilla resembles Little Spokane), so just the Klickitat and Little Spokane are shown.

The composites here clearly indicate the importance of the orography in determining precipitation amounts, with local maxima seen over the Cascade Mountain crest in both flow regimes. Some substantial differences in the character of the southwesterly and southeasterly associated distributions are nonetheless apparent. The southwesterly composites indicate a more widespread distribution of heavy rain than is seen during southeasterly flow. Particularly, the southwesterly/Klickitat result indicates that when it rains along the east flank of the Cascade Mountains it also tends to be quite wet not only over the Cascade crest and the coastal terrain (consistent with the expectation that enhanced orographic uplift associated with this flow regime will lead to widespread rainfall on the western Cascade slopes),

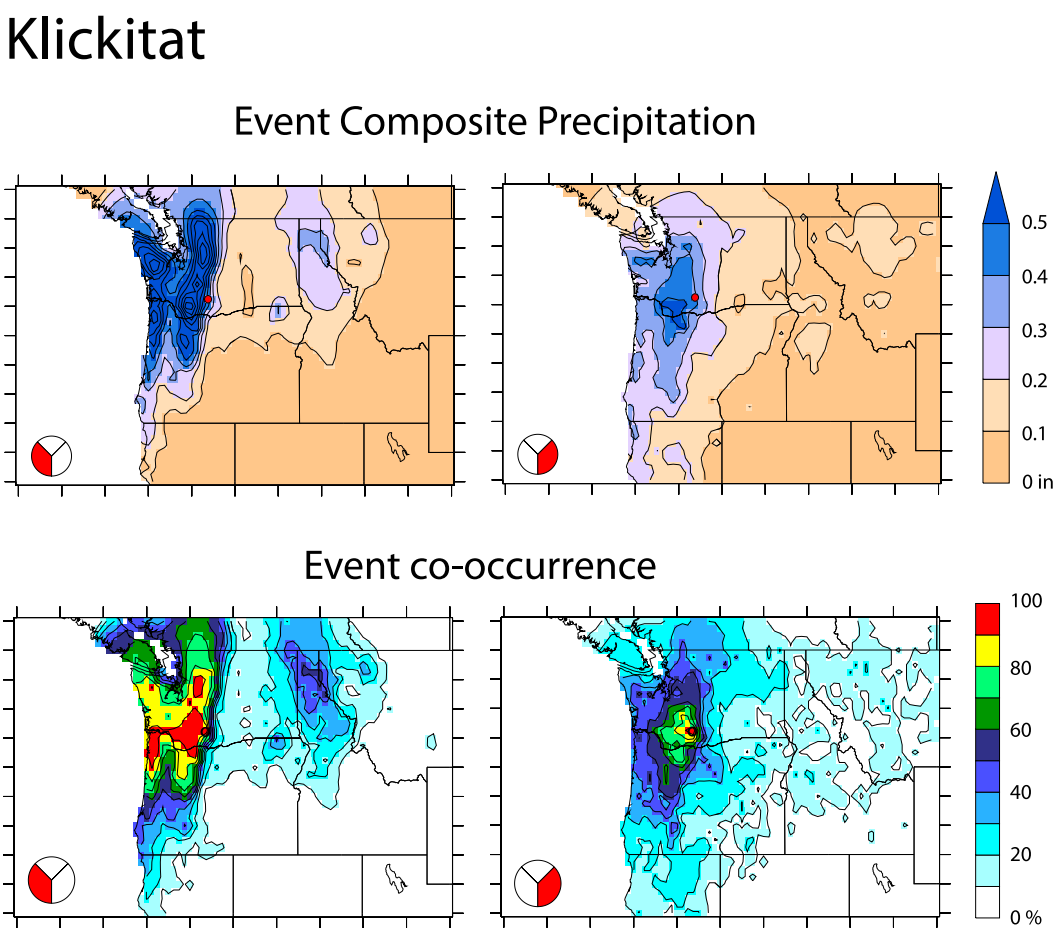

FIG. 11. (top) Composite average daily precipitation based on rainfall event days at the Klickitat site (location marked by a red dot). (bottom) Historical chance of seeing a co-occurring event at all other locations.

but also the higher elevations near the eastern Washington–Idaho border, ~400 km to the east of the Cascade crest. Conversely, the Cascades (including eastern slopes) and coastal terrain also tend to be wet during the days when rain events are seen at the Little Spokane site in this flow regime. This is broadly consistent with the analysis of Parker and Abatzoglou (2016), who found coherence in rainfall between the western slopes of the Cascade Mountains and the northern Rocky Mountains during the predominantly cool-season atmospheric river precipitation events considered therein. Chances are relatively good that when it rains on one of the mountainous flanks of the Columbia River basin in Washington during southwesterly flow conditions, the flank on the other side of the basin is wet as well.

The calculated probabilities of seeing a co-occurring rain event at other locations, based on the occurrence of a rain event at the Klickitat and Little Spokane sites, are shown in the bottom panels of Figs. 11 and 12, respectively. When a rain event occurs at the Little Spokane site in southwesterly flow, there is up to an 80% chance of also seeing a rain event along the Cascade Mountain crest (~400 km away). This chance drops below 50% in southeasterly flow.

10. Summary and discussion

This paper documents the characteristics of summertime rainfall events in the Pacific Northwest and examines their relationship to the prevailing regional midtropospheric circulation conditions. A particular focus of this work is on the forests of the interior Pacific Northwest, where these events can largely determine the start and end of the regional wildland fire season. A main result is that many event characteristics that are key from a forest management perspective (including location and the localization/spread of rainfall, as well as the likelihood of lightning) are closely linked to the prevailing midtropospheric circulation conditions, which may

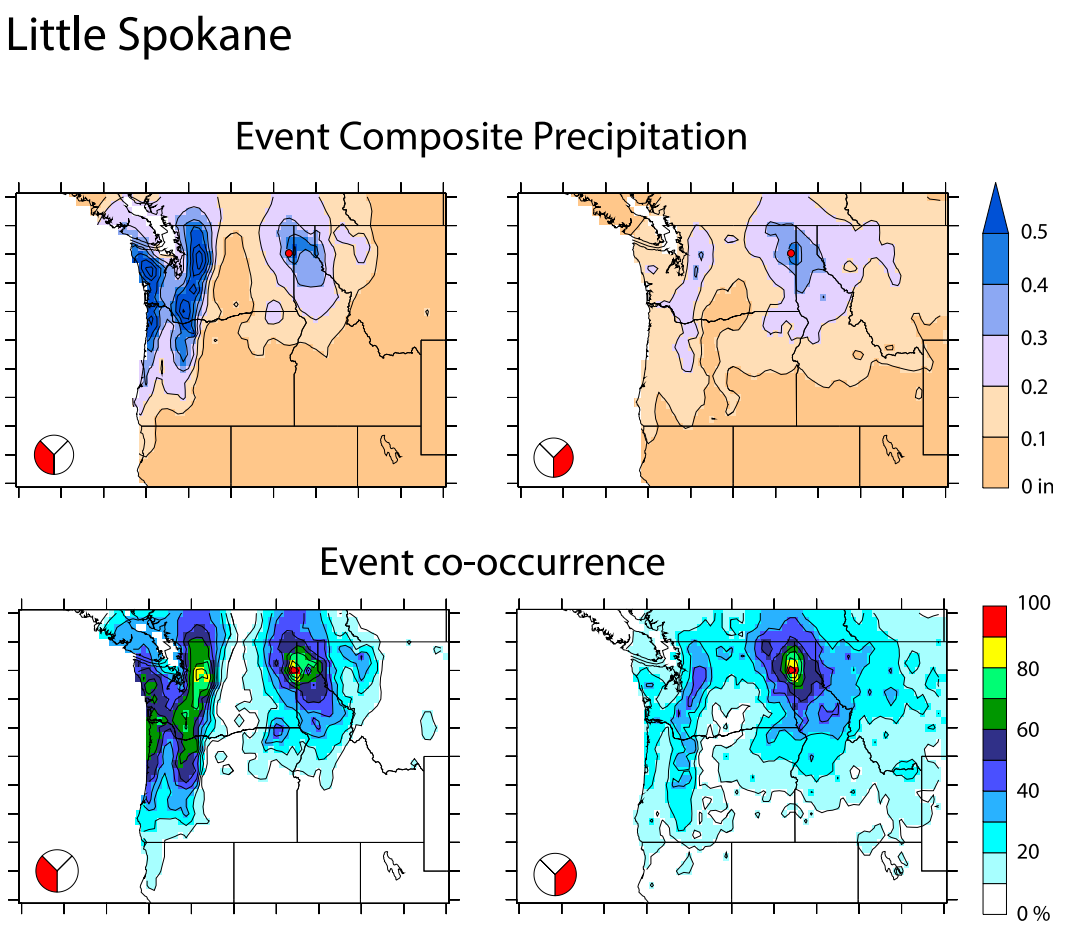

FIG. 12. As in Fig. 11, but for the Little Spokane River watershed.

now be forecasted with positive skill at lead times of a week and longer.

Rainfall events, as defined here, occur on average two to three times a summer (July–September) along the forested slopes of particular interest, with a minimum in late July. Events are more frequent than this along the crest of the Cascade Mountains and less frequent in the Columbia basin. A similar distribution is found for the magnitudes of these events in terms of the expected 20-yr maximum daily average summertime event rainfall. Streamflow observations for five selected watersheds all showed statistically significant day-to-day increases associated with the identified precipitation events, on average.

Precipitation events in the interior Pacific Northwest are rare during northerly flow anomalies and increase in frequency with more southerly flow, but whether the flow anomaly is southwesterly or southeasterly has a dramatic impact on the associated rainfall distribution pattern. The southwesterly flow events are associated with the majority of the events in the northwestern portion of the analysis domain and at higher elevations. Southwesterly events also primarily account for the minima in event frequency in late July. The southeasterly flow events account for most of the events in the lower elevations of the Columbia River basin and in the southern portion of the analysis domain. Southeasterly events are also associated with a considerably greater frequency of lightning strikes than southwesterly or northerly events. Southeasterly events also primarily account for the events in which lightning strikes were observed but rainfall was scarce. The spatial patterns in the frequency and magnitude of these events may be an important factor in determining differences in stream habitats and the mosaic of forest types. The lightning results, specifically that southeasterly events tend to be accompanied by considerably more lightning and less rainfall than events in other categories, have important connotations to wildland fire management and fire weather ignition predictions.

Composite event precipitation amounts exhibit enhancements over the higher elevations in all flow types, but heavy rains are more widespread in the southwesterly

events than the southeasterly events. Although rigorous study of the mechanisms responsible is beyond the scope of this work, we expect that these precipitation distribution differences are understandable from differences in the respective rainfall producing processes. Moisture (air parcel) trajectories over the North Pacific and orographic enhancement, at least on the west side of the Cascade Mountains, likely contribute to the heavier and more widespread rains seen in the southwesterly cases, which may be dominated by stratiform flow conditions that are not particularly conducive to deep convection and its spottier rainfall distributions. We suspect the southeasterly events to be more closely associated with dynamically driven convection and moisture pathways associated with the North American monsoon. It bears noting that the upper-tropospheric cutoff-low events, which were found by Abatzoglou (2016) to contribute substantially to regional summertime precipitation, are also not likely to be conducive to (western slope) orographic enhancement, and are apt to be included in the southeasterly events of the present study. Nonetheless, it came as a surprise to the authors that the southwesterly events account for as many summertime precipitation events on the east side of the Cascade Mountain crest as they do. We initially presumed that southeasterly events would represent the primary source of summertime rainfall east of the Cascade crest. However, about 60% of the summertime rainfall events seen at the Klickitat River site occurred in the southwesterly case, and even the focus sites located much farther (~400 km) east had at least 40% of the events in the southwesterly category.

That the rainfall events over the forests of particular interest here consist of a mix of southeasterly and southwesterly type 500-hPa flow events, along with the fact that these two types of events tend to have characteristically different rainfall distribution patterns, suggests that knowledge of the associated rainfall distribution characteristics (as described here), combined with skillful 500-hPa geopotential height forecasts, provides a useful basis for predicting the associated rainfall distribution aspects. The extended-range prediction horizon (as long as 4 weeks) stands out as one where immediate gains might be realizable. For example, the NOAA/CPC currently makes available 6–10-day, as well as 8–14-day, outlook maps of the 500-hPa geopotential height anomaly as well as precipitation. Experimental results out to 4 weeks from an ensemble of simulations by the Climate Forecast System (CFS) model are also available. The height anomaly outlooks are provided by the CPC with spatial resolution sufficient to determine the regional flow anomaly direction over the Pacific Northwest. The precipitation maps, however, are currently much more qualitative (e.g., predicting above, below, or normal chances of rain) and offered at spatial scales that are coarse compared to the steep terrain of interest here. Our results suggest that considering not just the precipitation outlooks, but also the 500-hPa geopotential height anomaly forecasts, will provide useful complementary information about how the upcoming events will distribute rain across the region. A pair of case examples that demonstrate the practical application of these results based on recent southeasterly and southwesterly events is provided in the supplementary material for this paper (available online at http://dx.doi.org/10.1175/WAF-D-16-0024.s1). Our results suggest that, on average, more localized rainfall distributions with relatively lower area-averaged accumulations over higher terrain and greater chances of lightning cooccurrence should be expected in the southeasterly case, along with more widespread and heavier distributions in the southwesterly case.

Some projections of much longer-term change might also be based on these results. Global climate change is expected to be accompanied by a poleward contraction of the hemispheric atmospheric circulation, and has been projected to be accompanied by reduced June–August-averaged precipitation over the U.S. northwest (Maloney et al. 2014) along with possible increases in consecutive dry days (Sillman et al. 2013). It is conceivable that one way in which the poleward circulation contraction might contribute to precipitation changes over this region is by causing the southwesterly flow events to become rare over a greater duration of the year, which essentially means a longer summer for the Pacific Northwest, as well as a longer and possibly more intense wildfire season.

Acknowledgments. This publication is funded by the U.S. Forest Service, with additional support for NAB and AMC by the Joint Institute for the Study of the Atmosphere and Ocean (JISAO) under NOAA Cooperative Agreements NA17RJ1232 and NA10OAR4320148. The authors thank J. Abatzoglou and two anonymous reviewers for helpful comments and suggestions and M. Rorig for help with the lightning data. AMC also acknowledges additional funding from the Climate Observations Division of the NOAA Climate Program Office.

REFERENCES

Abatzoglou, J. T., 2016: Contribution of cutoff lows to precipitation across the United States. *J. Appl. Meteor. Climatol.*, **55**, 893–899, doi:10.1175/JAMC-D-15-0255.1.

——, and C. A. Kolden, 2013: Relationships between climate and macroscale area burned in the western United States. *Int. J. Wildland Fire*, **22**, 1003–1020, doi:10.1071/WF13019.

——, ——, J. K. Balch, and B. A. Bradley, 2016: Controls on interannual variability in lightning-caused fire activity in the

western US. *Environ. Res. Lett.*, **11**, 045005, doi:10.1088/1748-9326/11/4/045005.

Bonnin, G. M., D. Martin, B. Lin, T. Parzybok, M. Yekta, and D. Riley, 2011: *Precipitation-Frequency Atlas of the United States*. NOAA Atlas 14, Vol. 1, NOAA/National Weather Service, Silver Spring, MD, 71 pp. + appendixes. [Available online at http://www.nws.noaa.gov/oh/hdsc/PF_documents/Atlas14_Volume2.pdf.]

Guirguis, K. J., and R. Avissar, 2008: An analysis of precipitation variability, persistence, and observational data uncertainty in the western United States. *J. Hydrometeor.*, **9**, 843–865, doi:10.1175/2008JHM972.1.

Higgins, R. W., W. Shi, E. Yarosh, and R. Joyce, 2000: *Improved United States Precipitation Quality Control System and Analysis.* NCEP/Climate Prediction Center Atlas 7, 40 pp. [Available online at http://www.cpc.ncep.noaa.gov/research_papers/ncep_cpc_atlas/7/toc.html.]

Kalnay, E., and Coauthors, 1996: The NCEP/NCAR 40-Year Reanalysis Project. *Bull. Amer. Meteor. Soc.*, **77**, 437–471, doi:10.1175/1520-0477(1996)077<0437:TNYRP>2.0.CO;2.

Lackmann, G. L., and J. R. Gyakum, 1999: Heavy cold-season precipitation in the northwestern United States: Synoptic climatology and analysis of the flood of 17–18 January 1986. *Wea. Forecasting*, **14**, 687–700, doi:10.1175/1520-0434(1999)014<0687:HCSPIT>2.0.CO;2.

Littell, J. S., D. McKenzie, D. L. Peterson, and A. L. Westerling, 2009: Climate and wildfire area burned in western U.S. ecoprovinces, 1916–2003. *Ecol. Appl.*, **1**, 1003–1021, doi:10.1890/07-1183.1.

Maloney, E. D., and Coauthors, 2014: North American climate in CMIP5 experiments: Part III: Assessment of twenty-first-century projections. *J. Climate*, **27**, 2230–2270, doi:10.1175/JCLI-D-13-00273.1.

Miller, J. F., R. H. Frederick, and R. J. Tracey, 1973: *Precipitation-Frequency Atlas of the Western United States*. NOAA Atlas 2, Vol. 9, NOAA/National Weather Service, 35 pp. [Available online at http://www.nws.noaa.gov/oh/hdsc/PF_documents/Atlas2_Volume9.pdf.]

NCEP/NCAR, 1996: NCEP/NCAR Reanalysis. NOAA Earth Systems Research Laboratory, accessed 1 March 2010. [Available online at http://www.esrl.noaa.gov/psd/data/gridded/data.ncep.reanalysis.html.]

Neiman, P. J., F. M. Ralph, G. A. Wick, J. Lundquist, and M. D. Dettinger, 2008: Meteorological characteristics and overland precipitation impacts of atmospheric rivers affecting the west coast of North America based on eight years of SSM/I satellite observations. *J. Hydrometeor.*, **9**, 22–47, doi:10.1175/2007JHM855.1.

——, L. J. Schick, F. M. Ralph, M. Hughes, and G. A. Wick, 2011: Flooding in western Washington: The connection to atmospheric rivers. *J. Hydrometeor.*, **12**, 1337–1358, doi:10.1175/2011JHM1358.1.

NLDN, 2002: National Lightning Detection Network data. Vaisala, accessed 21 May 2010.

NOAA, 2008: NOAA Climate Prediction Center U.S. Unified precipitation dataset. NOAA Earth Systems Research Laboratory, accessed 8 October 2009. [Available online at http://www.esrl.noaa.gov/psd/data/gridded/data.unified.html.]

Parker, L. E., and J. T. Abatzoglou, 2016: Spatial coherence of extreme precipitation events in the northwestern United States. *Int. J. Climatol.*, **36**, 2451–2460, doi:10.1002/joc.4504.

Rorig, M. L., and S. A. Ferguson, 1999: Characteristics of lightning and wildland fire ignition in the Pacific Northwest. *J. Appl. Meteor.*, **38**, 1565–1575, doi:10.1175/1520-0450(1999)038<1565:COLAWF>2.0.CO;2.

Rutz, J. J., W. J. Steenburgh, and F. M. Ralph, 2014: Climatological characteristics of atmospheric rivers and their inland penetration over the western United States. *Mon. Wea. Rev.*, **142**, 905–921, doi:10.1175/MWR-D-13-00168.1.

Sillmann, J., V. V. Kharin, F. W. Zwiers, X. Zhang, and D. Bronaugh, 2013: Climate extremes indices in the CMIP5 multimodel ensemble: Part 2. Future climate projections. *J. Geophys. Res. Atmos.*, **118**, 2473–2493, doi:10.1002/jgrd.50188.

USGS, 2009: USGS streamflow data. USGS Water Information System, accessed 28 October 2009. [Available online at http://waterdata.usgs.gov/nwis.]

van Wagtendonk, J. W., and D. R. Cayan, 2008: Temporal and spatial distribution of lightning in California in relation to large-scale weather patterns. *Fire Ecol.*, **4**, 34–56, doi:10.4996/fireecology.0401034.

Warner, M. D., C. F. Mass, and E. P. Salathé, 2012: Wintertime extreme precipitation events along the Pacific Northwest coast: Climatology and synoptic evolution. *Mon. Wea. Rev.*, **140**, 2021–2043, doi:10.1175/MWR-D-11-00197.1.